ADP-AT-99-7
Astropart. Phys. (submitted)

SN 1998bw–GRB 980425: A supernova explosion with a close massive companion?

R.J. Protheroe[1] and W. Bednarek[1,2]
[1]Department of Physics and Mathematical Physics
The University of Adelaide, Adelaide, Australia 5005.
rprother@physics.adelaide.edu.au
[2]University of Łódź, 90-236 Łódź, ul. Pomorska 149/153, Poland.
bednar@krysia.uni.lodz.pl

Abstract

Some gamma ray bursts may be produced by supernovae exploding in close massive binary systems (type Ib/c supernovae) as suggested by the recent observation of SN 1998bw/GRB 980425. We propose that high energy radiation observed in such gamma ray bursts may be produced by synchrotron radiation of electrons accelerated by 1st order Fermi acceleration at a quasi-stationary shock in the high velocity SN ejecta colliding with the companion star or some other nearby massive object. Nuclei would also be accelerated, and could give rise to an observable fluence of high energy neutrinos at Earth.

keywords: gamma-ray bursts – supernovae; acceleration mechanisms, gamma-rays, neutrinos, theory

1 Introduction

The gamma ray burst (GRB) source GRB 980425 was observed in low energy γ-rays by the OSSE [1] and Beppo-SAX detectors [2]. It was rather a weak burst with the spectrum being well described by a smoothly broken power law with a break at ~ 150 keV with a photon spectrum index above the break of -3.8 (i.e. essentially a cut-off) and an index below the break ranging from about -1 during the rise to about -2.6 during the decay [3]. From the observed fluence at 2–26 keV and 40–700 keV [4] we estimate an average photon index of ~ -1.9 during the burst which was of duration ~ 40 s [1]. This average photon spectrum index is close to -2 expected for complete cooling of an E^{-2} accelerated electron spectrum produced by shock acceleration.

Supernova 1998bw was discovered at a redshift 0.0085 to be within the error box of the GRB 980425 [3], and such a coincidence has been estimated as being very unlikely to occur by chance. This supernova was an unusual type Ib/c supernova with an estimated kinetic energy $\sim 3 \times 10^{52}$ erg [5], very strong radio emission, and had the highest ever observed expansion velocity of $v_{\rm s} = 60000$ km s^{-1}, even days after the explosion [6]. The identification of GRB 980425 with this supernova allows one to estimate the peak luminosity of the burst to be $\sim (5.5 \pm 0.7) \times 10^{46}$ erg s^{-1}, and its total 'γ-ray', or rather X-ray to hard X-ray, energy budget to be $(8.1 \pm 1.0) \times 10^{47}$ erg [3].

Models of GRB usually assume that the hard (> MeV) γ-ray emission observed in some GRB is produced by material moving with relativistic bulk motion with Lorentz factor $\sim 10^2 - 10^3$, either in the external medium [7] or during internal interactions of the moving plasma [8, 9]). If protons are accelerated in such highly relativistic flows, they should produce neutrinos with observable fluxes [9, 10, 11, 12]. Observations of extremely energetic and rapidly variable bursts at cosmological distances (e.g. GRB 971214 [13]; or GRB 990122 [14, 15]) indicate that sources of these bursts emit γ-rays highly anisotropically [16]. Possible scenarios for GRB sources have been recently proposed by Woosley in the collapsar model [17], Paczyński in the so called "hypernova" model [18], and Vietri & Stella in the SupraNova model [19]. In these models the formation of a rapidly spinning black hole or neutron star plays a basic role in production of highly relativistic anisotropic outflows (jets). However, at present there are no detailed models explaining how such highly relativistic jets can be produced, although such jets are known to occur in active galactic nuclei.

GRB 980425 seems to belong to the class of long duration GRB [20] with no hard γ-ray emission (about 25% in the BATSE sample [21]), and so the arguments requiring highly relativistic motion of the emission region do not apply to this object. Its energy in X-rays/hard X-rays is also orders of magnitude lower than the most energetic GRB observed. In fact, SN 1998bw, which is thought to produce this burst, showed unusually strong radio emission [22] but with a low level of polarization which might be interpreted as suggesting that the explosion was rather spherical, and did not involve highly collimated outflows.

It is believed that supernovae exploding in close massive binaries produce type Ib/c supernovae [23]. In this paper, we propose a model for GRB 980425 type bursts in which the presence of a massive companion star to a type Ib/c supernova plays an essential role. (Possible associations of GRB with supernovae SN Ib/c have been discussed in ref. [24]). The presence of dense matter very close to the burst origin, which is not expanding relativistically, is required by recent observations of iron lines from some GRB sources (e.g. GRB 970508 and GRB 970828 [25, 26]). Because these lines are not significantly blue-shifted they must be produced in the rest frame of the galaxy, and so could not be produced in the frame of a highly relativistic outflow. Meszaros and Rees [27] propose that an iron line may be produced on the surface of a close massive companion to the GRB (i.e. a massive supernova).

We suggest that electrons and nuclei may be accelerated at a stationary shock which

could occur as a result of the interaction of the high velocity component of the SN ejecta with the companion star. Very collimated high energy radiation may then be produced, for example, as a result of a highly anisotropic distribution of accelerated particles accelerated at a relativistic shock, or by the magnetic field and shock topology in the acceleration region. Provided the time available for acceleration since the formation of the shock is sufficient, the maximum energy occurs when the acceleration rate is balanced by losses, usually due to synchrotron emission in the case of electrons (also in the case of nuclei in one scenario we consider), and usually by pion production in collisions with matter in the case of nuclei. Radiation fields also provide potential photon targets for interaction of energetic electrons and nuclei, and we assume that the radiation field inside the acceleration region has two main components, thermal radiation from the surface of the companion star, and thermal radiation from the SN photosphere. Note that thermal radiation is observed in about 30% of GRB as soft X-ray precursors and tails with characteristic temperatures of 1-2 keV [28, 29].

In Section 2 we estimate the model parameters, discuss energetics, beaming, acceleration and interactions. In Section 3 we estimate the flux and fluence of high energy neutrinos. In Section 4 we further discuss our assumptions, and our conclusions are summarized in Section 5.

2 Model Parameters

In this section, we estimate the physical parameters of the model to determine the maximum energies of the accelerated particles, and the flux of high energy neutrinos resulting from subsequent hadronic interactions. First we shall use the observed GRB duration together with a model of the density of the SN ejecta to estimate the distance of the emission region of the X-ray to hard X-ray burst from the centre of the explosion under the assumption that the burst ends when the ejecta becomes optically thick to Compton scattering.

As the supernova shock wave moves outward through the pre-supernova star the outer layers are accelerated to become the supernova ejecta. The temperature of the fireball is typically a few 10^6 K at shock break out (see Table 2 in ref. [21]). However, as the ejecta homologously expands the photosphere radius rapidly increases and the temperature decreases. For an initially exponentially declining density profile, the density and Lorentz factors of the ejecta at radius r are related by

$$Q \approx \Gamma\beta(\rho r^3)^{0.2}, \tag{1}$$

where $Q = (3\text{–}4) \times 10^5$ g$^{0.2}$ is obtained from simulations of supernova explosions [21], Γ is the Lorentz factor of matter moving with velocity βc, ρ is the density of matter in g cm^{-3}, and r is the radial distance from the centre of the explosion in cm. We shall make the assumption that the ejecta is 100% fully ionized carbon in type Ib/c supernovae. Eq. 1 allows us to obtain the density of matter at the distance of the companion star $R_{\rm sep}$ as a

function of time t measured from the explosion,

$$\rho(t, R_{\rm sep}) = c^5 Q^5 [1 - (R_{\rm sep}/ct)^2]^{5/2} t^5 R_{\rm sep}^{-8}. \quad (2)$$

We use this density, for $Q = 3.5 \times 10^5$ g$^{0.2}$, to obtain the radius of the photosphere which we define to be the radius corresponding to unit Thomson optical depth from this radius to infinity ($\tau_T = 1$ for 5.1 g cm^{-2} of fully ionized carbon). In Fig. 1 we show the photosphere radius, $R_{\rm photo}$, as a function of time since the explosion.

We assume the photosphere emits black-body radiation, and so its temperature is given by

$$T_{\rm photo} = 1.94 \times 10^5 L_{42}^{1/4} R_{\rm photo,\,12}^{-1/2} \quad {\rm K} \quad (3)$$

where $L = 10^{42} L_{42}$ erg s^{-1} is the bolometric luminosity and $R_{\rm photo} = 10^{12} R_{\rm photo,\,12}$ cm. The bolometric luminosity of SN 1998bw was $\sim 1.7 \times 10^{42}$ erg s^{-1} shortly after the explosion (see fig. 3 of ref. [21]), giving the temperature of the photosphere as a function of time also shown in Fig. 1.

In Fig. 2 we show, as a function of distance from the centre of the explosion, i.e. the separation $R_{\rm sep}$ between the centre of pre-supernova star and the companion star, the time delay between the arrival of the fastest possible signal, $t_0 = R_{\rm sep}/c$, and the arrival of the photosphere at a later time, $t_{\rm photo}$. In our model, the GRB is produced near the companion star, and the arrival of the photosphere determines the end of the GRB emission because at that time the optical depth of escaping X-rays/hard X-rays to Compton scattering is 1, and subsequently rapidly increases. Clearly, for the model to be viable, the separation must be greater than the radius of the companion star. From Fig. 2, the observed burst duration of ~ 40 s implies a separation of 3.4×10^{12} cm, which satisfies this condition, unlike bursts of much shorter duration. Interestingly, this is of the same order of magnitude as close binary separations. We note that this distance scale also determines the time delay between the beginning of the UV flash, which is due to emergence of the SN shock wave from the surface of the pre-supernova star, and the beginning of the γ-ray burst which may occur when sufficient fast matter arrives at the companion star and shock acceleration begins. We therefore expect, as a natural consequence of our model, a correlation between the time delay of the GRB with respect to the UV flash and the duration of the GRB; longer GRBs should appear later after the UV flash. An early optical flash, with respect to the GRB, has been observed recently in the case of GRB990123 [30, 31], and may be a typical feature of GRBs.

Having estimated the distance of the GRB emission region from the pre-supernova star in the present model, we need next to determine the physical conditions there, and will start with the radiation field. We assume that the radiation field inside the acceleration region has two main components: thermal radiation from the surface of the companion star, and thermal radiation from the SN photosphere. Nonthermal radiation in the sub-MeV range will also be present during the burst duration, but for beaming factors obtained later, this will have too low a photon density to provide a significant target for interactions

of electrons or nuclei. For the thermal radiation from the surface of the companion star we assume black-body radiation with a temperature of 3×10^4 K, as being typical of OB stars.

We have already shown in Fig. 1 the temperature of the photosphere at time t (dashed curve), and it is seen to be below 1.5×10^5 K for $t > t_0$. However, the light received at the companion star at time t was emitted at an earlier time when the photosphere was hotter, and the solid angle subtended by the photosphere was smaller. We must therefore take care to include the light propagation times from the expanding photosphere as shown in Fig. 3. A photon emitted from the photosphere at point A at time t_1 arrives at the companion star at point B at time t_2 provided

$$\cos\theta = [R_{\rm sep}^2 + c^2(t_2 - t_1)^2 - R_{\rm photo}^2(t_1)]/[2R_{\rm sep}c(t_2 - t_1)]. \quad (4)$$

We show in Fig. 4 the maximum solid angle subtended by the photosphere, $\Omega_{\rm photo}$, for the maximum angle $\theta_{\rm max}$; we define the time of emission of light corresponding to $\theta_{\rm max}$ to be $t = t_{\rm emit}$. We show the temperature of the photosphere at time $t = t_{\rm emit}$, which we shall use for the thermal radiation from the SN photosphere assuming a black-body spectrum with temperature $T = T_{\rm photo}(t_{\rm emit})$ but diluted by factor $\Omega_{\rm photo}/4\pi$.

We must make some assumption to determine the magnetic field to be used in the acceleration and synchrotron radiation processes. Since we are interested in knowing the magnetic field at times before the SN photosphere has reached the companion star, it seems unreasonable to argue that it is in equi-partition with the SN thermal radiation field. Instead we shall consider the likely location of the shock in relation to the companion star, and this will depend on the ram pressure of the arriving SN ejecta, $p_{\rm ram} = (\rho\gamma\beta c)(\beta c)$. We will then be in a better position to decide on the most appropriate magnetic field.

The fastest possible matter reaches the companion star at $t = t_0 \equiv R_{\rm sep}/c$, and matter with velocity βc will reach the star at time $t = R_{\rm sep}/\beta c$. The estimated burst duration, $\Delta t_{\rm GRB} \approx 40$ s then allows us to determine minimum velocities of SN ejecta near the companion star over the duration of the GRB,

$$\beta > \beta_{\rm min} = t_0/(t_0 + \Delta t_{\rm GRB}) \approx 0.74, \quad (5)$$

corresponding to Lorentz factors $\Gamma > \Gamma_{\rm min} = 1.48$. The Lorentz factors of matter arriving at $r = R_{\rm sep}$ are plotted as a function of $(t - t_0)$ in Fig. 5. The density and ram pressure are plotted in Fig. 6. The ram pressures plotted far exceed those present in the stellar wind of a typical OB star, and also exceeds a magnetic pressure of $\sim 4 \times 10^4$ erg cm^{-3} corresponding to a stellar surface magnetic field of 10^3 G. The shock will therefore be near to the stellar surface, and extend around and beyond the star. We expect that the SN ejecta, being ionized, is able to compress the star's dipole magnetic field until its magnetic pressure balances the ram pressure. The shock would then occur at a height

$$h_{\rm shock} \approx 0.5 R_{\rm star} B_{\rm star}/B_{\rm ram} \quad (6)$$

above the surface of the star, where $R_{\rm star} \sim 10^{12}$ cm is typical of the radii of OB stars, $B_{\rm star} \sim 10^3$ G is a reasonable surface magnetic field for OB stars, and $B_{\rm ram} \sim \sqrt{8\pi p_{\rm ram}}$.

For the ram pressures at $(t - t_0) = 1$ s, 10 s, and 100 s, the shock height would be $h_{\rm shock} \sim 1.6 \times 10^{-2} R_{\rm star}$, $1.6 \times 10^{-3} R_{\rm star}$, and $1.5 \times 10^{-4} R_{\rm star}$, respectively. If, as seems less likely to us, the dipole field were not efficiently compressed the shock would occur deep in the stellar atmosphere, and shock acceleration would be quenched by energy losses due to interactions with matter. However, around the sides of the star the density at the shock would be lower, and shock acceleration may proceed in magnetic field $B \sim B_{\rm star}$. We therefore consider two possible values of the magnetic field: $B \sim 10^3$ G as at the stellar surface, and $B \sim \sqrt{8\pi p_{\rm ram}}$.

2.1 Synchrotron radiation by electrons

In our model, the X-ray to hard X-ray burst is due to synchrotron radiation by electrons in a region of comparable size to the companion star. Before going further, we should first check whether synchrotron self-absorption for the assumed magnetic fields of 10^3 G, and $\sim 10^6$ G at $(t - t_0) = 40$ s, is likely to present any problems for the model.

The optical depth for photons with frequency ν (in Hz) is given by [32]

$$\tau_{\rm ss} = 0.019 L (3.5 \times 10^9)^{\gamma} K B^{(\gamma+2)/2} \nu^{-(\gamma+4)/2}, \tag{7}$$

where L is the extent of the source along the line of sight, $\gamma \sim 2.8$ is the power law spectral index of electrons in the source which we infer from the average photon spectrum index of 1.9 (see Section 1). The constant K is

$$K = 7.4 \times 10^{21} (I_\nu / LB) (\nu / 6.26 \times 10^{18})^{(\gamma-1)/2}, \tag{8}$$

where I_ν is the intensity of synchrotron photons at frequency ν (in erg cm^{-2} Hz^{-1} s^{-1} sr^{-1}). Assuming that photons are absorbed when $\tau_{\rm ss}$ is greater than one, we estimate that photons with frequency,

$$\nu < 1.5 \times 10^{13} I_\nu^{2/5}, \tag{9}$$

are absorbed for $B = 10^6$ G. The intensity of synchrotron photons at the source is related to the differential photon flux observed from GRB 980425, $F_\nu \approx 2.8 \times 10^{-10} \nu^{-0.9}$ erg cm^{-2} Hz^{-1} s^{-1}, through

$$F_\nu = I_\nu \frac{S}{D^2}, \tag{10}$$

where S is the projected area of the source of synchrotron photons, and D is the source distance. From Eqs. (9) and (10), we find that if the emission area of 1 keV synchrotron photons is larger than $\sim 2.7 \times 10^{16}$ cm^2, i.e. $\sim 10^{-8} \pi R_{\rm star}^2$, the photons are not self absorbed. This limit is less restrictive for 10^3 G ($\sim 8.5 \times 10^{14}$ cm^2), and so we can reasonably neglect synchrotron self-absorption.

We next check that the Razin effect (see e.g. [33]) could give rise to a low energy cut-off in the X-ray flux during the GRB. With an electron number density in the SN

ejecta $n_e \approx \rho/2m_p \sim 10^{13}$ cm^{-3} at $(t - t_0) = 40$ s, we find the Razin effect cut-off would be below 1 keV provided $B > 4 \times 10^{-3}$ G, and again we can safely neglect this.

We assume acceleration of electrons and protons occurs at a shock created by the interaction of the SN ejecta and the binary companion star at a rate

$$dE/dt = \eta Ec/r_g \approx 9 \times 10^3 B \quad \text{GeV s}^{-1} \tag{11}$$

where η is the acceleration rate parameter, r_g is the gyroradius, and B is in Gauss. (Note that although nuclei other than protons would be accelerated if present, in this paper we shall only consider the consequences of acceleration of protons).

The value of the acceleration rate paramenter η can be determined from the assumption that the maximum energy of the GRB spectrum is determined by a balance between energy gains and synchrotron losses. The maximum Lorentz factor of electrons accelerated in magnetic field B is

$$\gamma_{\rm e,max} \approx 1.2 \times 10^6 \eta^{1/2} B^{-1/2}. \tag{12}$$

GRB spectra usually have a break in their spectrum close to a few hundred keV and in the case of GRB 980425 the break is at $\epsilon_{\rm max} \sim 150$ keV; the spectrum cuts-off steeply above this energy. Photons with this energy are produced by primary electrons with Lorentz factors given by Eq. 12,

$$\epsilon_{\rm max} = m_{\rm e} c^2 \frac{B}{B^e_{\rm cr}} \gamma^2_{\rm e,max} \approx 300 m_{\rm e} c^2 \eta \tag{13}$$

where $B^e_{\rm cr} = 4.4 \times 10^{13}$ G. From this equation we can uniquely estimate the value of the acceleration rate parameter,

$$\eta \approx 10^{-3}, \tag{14}$$

and this is independent of the assumed magnetic field.

2.2 Energetics and beaming

We assume an injection spectrum of electrons of the form

$$\dot{N}_e(E,t) \approx (1+\zeta)^{-1} \xi k P_{\rm kin}(t) E^{-2} / \ln(\gamma_{\rm e,max}/2), \tag{15}$$

from $E = 2m_e c^2$ up to the cut-off energy $\gamma_{\rm e,max} m_e c^2$, where ζ is the electron to proton ratio, ξ is a factor for the efficiency of conversion of kinetic energy of SN ejecta into ultra-relativistic particles at the shock, $k \approx \pi R^2_{\rm star}/4\pi R^2_{\rm sep}$ gives the fraction of the SN ejecta intercepted by the shock at the companion star, and $P_{\rm kin}(t)$ is the kinetic energy flux through a sphere of radius $R_{\rm sep} = 3.4 \times 10^{12}$ cm centred on the explosion at time t. The kinetic energy flux, $P_{\rm kin}(t)$, is plotted against time in Fig. 7 as the solid curve.

For an E^{-2} injection spectrum of electrons, complete cooling by synchrotron radiation will produce an ε^{-2} photon spectrum, as required. The total power in the synchrotron emission will then be close to the total power injected in relativistic electrons. The observed synchrotron power will depend on the beaming of electrons in the observer's frame, which will also be the shock frame for a quasi-stationary shock (neglecting the small effect due to the redshift of SN 1998bw). For $(t-t_0) < 100$ s the shock is relativistic, and the distribution of accelerated particles will be highly anisotropic. Typical angles of particles returning from upstream to the shock are $\sim \sqrt{2}/\Gamma$ as measured in the upstream frame [34] which is also the frame of the SN ejecta at the shock. Transforming to the shock frame (observer's frame) we find typical angles $\theta_{\rm beam} \sim 1/\sqrt{2}\Gamma^2$. Hence the beaming solid angle will be $\Omega_{\rm beam} = 2\pi(1-\cos\theta_{\rm beam}) \sim \pi/2\Gamma^4$.

We have added to Fig. 7 the product of the kinetic energy flux, the fraction of the SN ejecta intercepted by the shock at the companion star, and the beaming factor $4\pi/\Omega_{\rm beam} = 2/(1-\cos\theta_{\rm beam}) \sim 8\Gamma^4$. We see that the resulting 'apparent kinetic energy flux' available (dashed curve) is approximately constant at $\sim 10^{47}$ erg s^{-1} while the shock is relativistic, and then increases with time. This is interestingly of the right order of magnitude, about a factor of 4 higher than that observed for the X-ray to hard X-ray emission during the ~ 40 s of the burst, but implying a very high efficiency, $\xi \sim 0.5$. Nevertheless, we find it encouraging as the model will be sensitive to the input parameters, and it may well be possible to obtain agreement with the data with more reasonable energy conversion efficiencies for different input assumptions for the SN explosion parameters and shock geometry. From now on, we will assume that the apparent kinetic energy flux available has the energy dependence as given by the dashed curve in Fig. 7, and is normalized such that for $(t-t_0) < 100$ s it is equal to the estimated peak luminosity of GRB 980425 multiplied by $(1+1/\zeta)$ where ζ is the electron to proton ratio.

2.3 Acceleration and interaction of electrons and protons

We next estimate the maximum energies of electrons and protons accelerated at a shock near the companion star at various times later than t_0. We show time scales for acceleration, and various loss processes, in Fig. 8 for $B = 10^3$ G, and in Fig. 9 for $B = \sqrt{8\pi p_{\rm ram}}$. Each figure has four parts corresponding to the following times: (a) $(t-t_0) = 1$ s, (b) $(t-t_0) = 10$ s, (c) $(t-t_0) = 100$ s, and (d) $(t-t_0) = 1000$ s. For acceleration we assume $\eta \approx 10^{-3}$. For interactions with matter (bremsstrahlung and Coulomb/ionization interactions by electrons, pion production interactions of protons with nuclei, i.e. 'pN' interactions) we use the density given in Fig. 6 and assume a composition of 100% carbon, taken to be fully ionized when calculating bremsstrahlung and Coulomb/ionization losses [36]. We base the energy dependent p-Carbon nucleus cross section we use on the p-air nucleus cross section [35]. For interactions with radiation (inverse Compton scattering by electrons, and Bethe-Heitler pair production, and pion photoproduction by protons – see e.g. [37, 38]) we consider two components of the radiation field: 3×10^4 K black-body starlight component, and diluted thermal radiation from the SN photosphere as discussed

previously. Time scales for all these processes are shown in Figs. 8 and 9, together with the time available for acceleration and interaction processes to occur, i.e. $(t - t_0)$. The maximum energies, the loss processes responsible for the cut-offs, and the emission processes of the accelerated electron and proton populations are summarized in Tables 1 and 2 for $B = 10^3$ G, and $B = \sqrt{8\pi p_{\rm ram}}$, respectively.

Table 1: Maximum energies (GeV), cause of cut-off in spectrum, and emission processes of electrons and protons for $B = 10^3$ G and $\xi = 10^{-3}$ at distance $r = 3.4 \times 10^{12}$ cm.

$t - t_0$ (s)	$E^e_{\rm max}$	Cause/Process	$E^p_{\rm max}$	Cause	Process
0.32	60	Syn.	2.5×10^3	Time	pN after ~ 30 s
1.0	60	Syn.	8.0×10^3	Time	pN after ~ 30 s
3.2	60	Syn.	2.5×10^4	Time	pN after ~ 30 s
10.0	60	Syn.	10^5	Time	pN after ~ 30 s
31.6	60	Syn.	1.5×10^5	pN	pN
100	60	Syn.	1.3×10^4	pN	pN
316	10	Bremss.	200	pN	pN
1000	0.1	Bremss.	2	pN	pN
3160	0	Bremss.	0	pN	pN

3 Results

Using the normalization for the proton spectrum described above, and assuming $\zeta = 1$, we have obtained the $(\nu_\mu + \bar{\nu}_\mu)$ flux at Earth for E^{-2} proton spectra extending up to the maximum energies of protons that will interact by pion production interactions with nuclei as given in Tables 1 and 2. For this we have used recent parametrizations of cross sections for γ-ray and $e^\pm$ production resulting from pp interactions followed by pion decay [39] appropriately scaled for $(\nu_\mu + \bar{\nu}_\mu)$ production. Results are shown in Fig. 10 for (a) $B = 10^3$ G, and (b) $B^2/8\pi = p_{\rm ram}$. As can be seen, the higher magnetic field model with $B^2/8\pi = p_{\rm ram}$ gives higher proton and neutrino energies, and a longer duration neutrino burst. We have neglected the effect of synchrotron losses of muons before they decay as this has an almost negligible effect on our results — only the 300 s curve in Fig. 10(b) would change with a cut off at about a factor of 2 lower in energy than shown.

In Fig. 11(a) we show the $(\nu_\mu + \bar{\nu}_\mu)$ fluences for the two assumptions about B. In order to determine whether or not the fluences predicted are likely to be observable with the next generation of neutrino telescopes, which are planned to have areas approaching 1 km^2, we estimated the muon signal expected in a 1 km^2 detector. We have estimated the number of events as a function of minimum muon energy using the $P_{\nu\to\mu}(E_\nu, E_\mu^{\rm min})$ function given in fig. 2 of ref. [40] for $E_\mu^{\rm min} = 1$ GeV, modified for other $E_\mu^{\rm min}$ values in a way consistent

Table 2: Magnetic field, maximum energies (GeV) of electrons (due to synchroton loss) and protons, cause of proton spectrum cut-off, and proton interaction processes (energy range in GeV, time of emission in s) for $B^2/8\pi = p_{\rm ram}$ and $\xi = 10^{-3}$ at distance $r = 3.4 \times 10^{12}$ cm.

$t - t_0$ (s)	B (G)	$E^e_{\rm max}$	$E^p_{\rm max}$	Cause	Process (energy range, time)
0.32	10^4	20	3×10^4	Time	pN ($<3\times10^4$, ~ 32)
1.0	3.2×10^4	10	2.5×10^5	Time	pN ($<10^5$, ~ 32); Syn. ($>10^5$, ~ 32)
3.2	10^5	6	3×10^6	Time	pN ($<10^5$, ~ 32); Syn. ($>10^5$, ~ 32)
10.0	3.2×10^5	3	10^7	Syn.	pN ($<10^5$, ~ 32); Syn. ($>10^5$, ~ 32)
31.6	10^6	1.5	7×10^6	Syn.	pN ($<10^5$, ~ 32); Syn. ($>10^5$, ~ 32)
100	3.2×10^6	1	3×10^6	Syn.	pN ($<3\times10^5$, 100); Syn. ($>3\times10^5$, 100)
316	1.3×10^7	0.5	10^6	Syn.	pN ($<10^6$, 316)
1000	5×10^7	0.25	10^5	pN	pN ($<10^5$, 1000)
3160	2.5×10^8	0.1	10^3	pN	pN ($<10^3$, 3160)

with that given for $E_\mu^{\rm min} = 1$ TeV. The effects of shadowing for vertically upward-going neutrinos have been included using the shadow factor $S(E_\nu)$ given in fig. 20 of ref. [41]. The expected neutrino induced muon signal for the horizontal and vertical directions corresponding to the neutrino fluences shown in Fig. 11(a) are shown in Fig. 11(b) where they are compared with the atmospheric neutrino background expected during 100 s within 5° of the source direction. We see that for GRB 980425 we would expect ~ 3 muons above 1 TeV if $B^2/8\pi = p_{\rm ram}$, and $\sim 5 \times 10^{-3}$ muons if $B = 10^3$ G. For nearer or more powerful GRB—SN Ib/c associations, the signal expected would be higher.

4 Discussion

Since the beaming arising from relativistic shock acceleration seems to be a necessary requirement for the GRB to be observable in our model, we discuss this now in more detail. In the case of a plane relativistic shock it has been shown that typical angles of upstream particles on returning to the shock are $\sim \sqrt{2}/\Gamma$ as measured in the upstream frame which is also the frame of the SN ejecta, and this result appears to be almost independent of the scattering mechanism, if any (see e.g. ref. [34]). Thus, in the shock frame (the observer's frame in the case of the present model) the beaming solid angle would be $\Omega_{\rm beam} \sim \pi/2\Gamma^4$. For high shock Lorentz factors, shock acceleration can therefore essentially produce a beam of accelerated particles with a very narrow angular spread. The accelerated electrons will radiate by synchrotron emission, and for injection of a parallel beam of electrons of energy $\gamma_e m_e c^2$ into a regular magnetic field at pitch angle θ, the synchrotron emission will be beamed into solid angle $\Omega_{\rm syn} \approx 4\pi \sin(\theta) \sin(1/\gamma_e)$.

Examining Figs. 8(a)-(b) and 9(a)-(b) we see that typical values of γ_e that will contribute to synchrotron emission of the X-ray to hard X-ray burst are 10^5 and 10^4, respectively. Thus the intrinsic beaming due to the synchrotron process is narrower than that of the accelerated particle beam for $(t - t_0) > 1$ s, and our use of $\Omega_{\rm beam} \sim \pi/2\Gamma^4$ appears to be appropriate. Realistically, the shock geometry may be oblique or perpendicular, and will be changing as the ram pressure changes with time. This may give rise to special effects analogous to apparent superluminal motion/beaming which may be present in AGN, or superluminal acceleration [42] and shock drift acceleration which could possibly enhance the beaming. Also, one should not forget that the companion star itself, and therefore the shock, will be moving and this may modify the observed time dependence of any observed flux. In addition, during the synchrotron process, it is the component of momentum perpendicular to the field direction which is cooled, giving rise to a further beaming in the field direction for the lower energy electrons, and the field direction may well be approximately in the direction of ejecta flow around the sides of the companion star beaming the synchrotron radiation in that direction. Clearly beaming is a complicated topic, and a full discussion is beyond the scope of the present paper. However, it does seem plausible to us that the synchrotron radiation and high energy neutrinos from pN collisions may be sufficiently beamed in our model for them to be potentially observable from sources such as GRB 980425/SN 1998bw.

We next discuss the consequences of the assumed beaming to the statistics of the association of GRB and SN type Ib/c. We note that the beaming solid angle increases dramatically as the ejecta arriving at the shock changes from relativistic to mildly relativistic towards the end of the GRB. If the line of sight to the GRB is not well aligned with the beaming direction, the start of the observed burst may be delayed somewhat until the beaming angle expands to include our line of sight. However, towards the end of the burst (defined by $\tau_T = 1$) the ejecta has slowed sufficiently such the beaming solid angle is reasonably large. In the case of the shock at 3.4×10^{12} cm, $\Omega_{\rm beam} = 0.34$ sr at $(t - t_0) = 40$ s. The burst duration would be different for different binary separations, and $\Omega_{\rm beam}$ at the end of the burst duration would vary. We estimate that for burst durations of 1 s, 10 s and 100 s, the final beaming solid angle would be 0.17 sr, 0.5 sr, and 0.96 sr, respectively. Assuming that all SN Ib/c produce anisotropically GRB of this type, and applying a rate of SN Ib/c explosions per galaxy of ~ 1 per 100 years, and a galaxy density $\sim 1.7 \times 10^{-2}$ Mpc^{-3} [45], we estimate that $\sim 3\Omega_{\rm beam}$ SN Ib/c type supernovae closer than GRB 980425 should be observed per year in association with long-duration GRBs.

In proton-nucleus collisions producing neutrinos through $\pi \to \mu \to e$ decay, electrons will be produced, and γ-rays will result from π^0 decay. However, because the mean interaction time decreases very rapidly with $(t - t_0)$, pN collisions are rare until $(t - t_0) \sim$ 30–40 s when the mean interaction time becomes comparable to $(t - t_0)$. At this time, the emission region is almost optically thick to X-rays and low energy γ-rays ($\tau_T \sim 1$), and is rapidly becoming optically thick to high energy γ-rays (note also that the pair production cross section in fully ionized matter has a strong logarithmic energy dependence), and

so whether these γ-rays will escape is questionable, and their subsequent cascading may be of little consequence apart from returning energy to the ejecta as heat. However, if these proton-nucleus collisions contribute to the X-ray to low energy γ-ray burst signal near the end of the burst, the emerging photons will mainly result from a magnetic pair production synchrotron cascade [43]. Such cascades may be important in active galactic nuclei [44]. Since the mean free path for γ-rays in the higher magnetic field model is very short, the cascade would saturate very rapidly. This process degrades the highest energy γ-rays and pairs to energies in the range $\sim 1 - 10$ TeV. Gamma-ray photons with these energies are absorbed on the black body photons in the source region creating $e^{\pm}$ pairs with similar energies. The pairs with such energies cool predominantly by synchrotron radiation (see Fig. 9). As a result of such a cascade much of the initial energy of photons and $e^{\pm}$ from pion decay is transferred into photons with energies below electron rest mass and may contribute to the final stages of the X-ray to low energy γ-ray emission in some GRBs. However, in some GRB—SN type Ib/c associations 100 MeV–GeV γ-rays could be produced towards the end of the burst.

So far we have neglected synchrotron radiation by protons other than as an energy loss process in determining the maximum proton energy, and in determining up to what energy an accelerated proton spectrum will interact by proton-nucleus collisions (see Table 2). In the case of $B^2/8\pi = p_{\rm ram}$, synchrotron radiation may give rise to observable photons after $(t - t_0) \sim$ 10–100 s (depending on proton energy) when synchrotron cooling becomes efficient. Those photons produced with high energies will suffer the same fate as those produced by π^0 decay at high energies described above. Examining Fig. 9(b) we see that protons produced at $(t - t_0) \sim 10$ s with energies between $\sim 3 \times 10^6$–10^7 GeV will cool efficiently in a 3×10^5 G field and could give a contribution in the keV range. As the magnetic field rapidly increases with time in this model, contributions at later times would be at higher energies and would cascade as described earlier.

As we noted in the introduction, the UV flash should precede the GRB which would only start when sufficient SN ejecta reached the region of the companion star. We estimate the time delay between the beginning of the UV flash and the maximum of the GRB flux to be

$$t_{\rm delay} \approx (1 - \beta_{\rm min}) R_{\rm sep}/c. \tag{16}$$

For $\beta_{\rm min} = 0.74$ as estimated for GRB 980425 this delay is $t_{\rm delay} \approx 30$ s. For similar GRB the delay will depend on the separation of the companion stars. Note that the separation of the stars determines also the burst duration (see Fig. 2), and so our model predicts a correlation between the GRB duration and the time delay between the beginning of the UV flash and the maximum of the GRB flux.

We should mention that nuclei other than protons may well be accelerated at the shock, particularly if the metal-rich SN ejecta itself is injected into the acceleration process. Since the acceleration process actually depends on magnetic rigidity (momentum divided by charge), it may well be possible for nuclei to be accelerated to somewhat higher energies. How this would affect the predicted neutrino signals may be left to a later paper.

Finally, we note that a shock in the SN ejecta could be caused instead by the presence of a nearby massive dense cloud, or perhaps by the presence of piled-up stellar wind material in the vicinity the pre-supernova star due to its stellar wind colliding with a nearby dense object. Depending on the physical conditions, the resulting relativistic shock in the SN ejecta may accelerate particles and produce an observable X-ray to hard X-ray burst, and neutrino signal, in a way similar to that discussed in the present paper.

5 Conclusion

We have developed an alternative model of low-power long-duration GRB associated with type Ib/c supernovae in which the X-ray to hard X-ray emission is produced as synchrotron radiation by electrons accelerated at a shock in the SN ejecta caused by the presence of a binary companion star to the pre-supernova star. In our model, the burst duration fixes the location of the shock in GRB 980425/SN 1998bw to be at $\sim 3 \times 10^{12}$ cm which is a reasonable binary separation. Nuclei will also be accelerated, and if the magnetic field is in equi-partition with the ram pressure of the SN ejecta at the shock, this could result in an observable muon signal in proposed km^2 high energy neutrino detectors.

Acknowledgements

We would like to thank Anita Mücke for valuable discussions and Qinghuan Luo for reading the manuscript. W.B. thanks the Department of Physics and Mathematical Physics at the University of Adelaide for hospitality during his visit. This research is supported by a grant from the Australian Research Council and by the Polish Komitet Badań Naukowych grant 2P03D 001 14.

References

[1] Kippen, R.M. and the BATSE Team, 1998, GCN Circ. 67, http://lheawww.gsfc.nasa.gov/docs/gamcosray/legr/bacodine/gcn3/067.gcn3

[2] Soffitta P. et al., 1998, IAU Circ. No. 6884

[3] Galama T.J. et al., 1998, Nature, 395, 670

[4] Pian, E., et al., 1999, astro-ph/9903113

[5] Iwamoto K. et al., 1998 Nature, 395, 672

[6] Stathakis R.A. et al., 1999, in preparation (see ref. [22])

[7] Meszaros, P., Rees, M.J., 1993, ApJ, 405, 278

[8] Rees, M.J., Meszaros, P., 1994, ApJ, 430, L93

[9] Paczyński, B., Xu, G., 1994, ApJ, 427, 708

[10] Waxman, E., Bahcall, J., 1997, Phys.Rev.Lett., 78, 2292

[11] Vietri, M., 1998, Phys.Rev.Lett., 80, 3690

[12] Rachen, J.P., Meszaros, P., 1998, Phys.Rev. D, 58, 123005

[13] Kulkarni, S.R. et al., 1998, Nature, 393, 35

[14] Kelson, D.D. et al. 1999, IAU Circ. 7096

[15] Kippen, R.M. and the BATSE Team, 1999, GCN Circ. 224

[16] Dar A., Plaga R., 1999, A&A, submitted, astro-ph/9902138

[17] Woosley, S.E., 1993, ApJ, 405, 273

[18] Paczyński, B., 1998, ApJ, 484, L45

[19] Vietri, M., Stella, L., 1998, ApJ, 507, L45

[20] Kouveliotou, C. et al., 1993, ApJ, 413, L101

[21] Woosley, S. E., Eastman, R.G., Schmidt, B.P., 1998, ApJ, submitted, astro-ph/9806299

[22] Kulkarni S.R. et al., 1998, Nature, 395, 663

[23] Nomoto, K., Fillipienko, A.V., Shigeyama, T., 1990, A&A, 240, L1

[24] Wang L., Wheeler J.C., 1998, ApJ 504, L87

[25] Piro. L. et al., 1999, ApJ, 514, L73

[26] Yoshida A. et al., 1999, ApJ, submitted

[27] Meszaros P., Rees, M.J., 1998, MNRAS, 299, L10

[28] Murakami T. et al., 1991, Nature, 350, 592

[29] Sazonov S.Y. et al., 1998, A&ASuppl., 129, 1

[30] Akerlof, C.W., and McKay, T.A., 1999, IAU Circ. 7100

[31] Fenimore E.E., Ramirez-Ruiz E., Wu B., 1999, ApJ, submitted, astro-ph/9902007

[32] Lang, K.R., 1980, Astrophysical Formulae (Springer-Verlag)

[33] Rybicki, G.B., and Lightman, A.P., 1979, Radiation Processes in Astrophysics (Wiley, New York)

[34] Gallant Y.A. and Achterberg A., 1999, MNRAS (Letters), in press.

[35] Gaisser, T.K., 1990, Cosmic Rays and Particle Physics, (Cambridge University Press, Cambridge)

[36] Ginzburg, V.L., and Syrovatskii, S.I., 1964, The Origin of Cosmic Rays (Pergamon Press, Oxford).

[37] Protheroe, R.J., 1986, Mon. Not. R. Astron. Soc., 221, 769

[38] Protheroe, R.J., and Johnson, P.A., 1995, Astroparticle Phys., 4, 253

[39] Moskalenko, I.V., Strong, A.W., 1998, ApJ, 493, 694

[40] Gaisser, T.K., Halzen, F., Stanev, T., 1995, Phys.Rep. 258, 173

[41] Gandhi, R., Quigg, C., Reno, M.H., Sarcevic, I., 1998, Phys. Rev. D58 (1998) 093009

[42] Begelman M.C., Kirk J.G., 1990 ApJ, 353, 66

[43] Erber, T., 1966, Rev.Mod.Phys., 38, 626

[44] Bednarek, W., Protheroe, R.J., 1999, MNRAS, 302, 373

[45] Binney, J., Tremaine, S., 1987, Galactic Dynamics (Princeton University Press, Princeton)

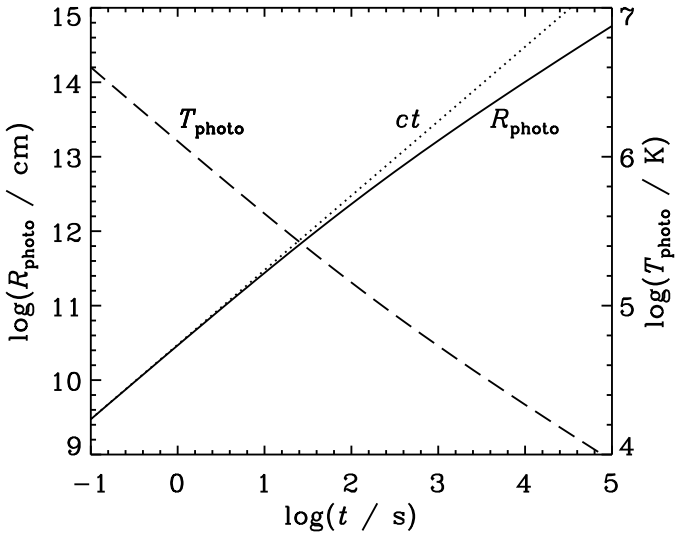

Figure 1: Radius and temperature of the photosphere as a function of time after the explosion.

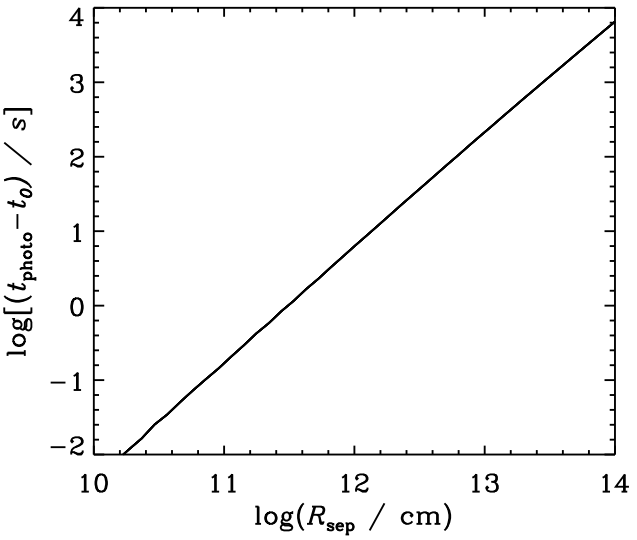

Figure 2: Time delay between arrival of fastest matter ($v \to c$) and arrival of photosphere as a function of distance from the centre of the explosion.

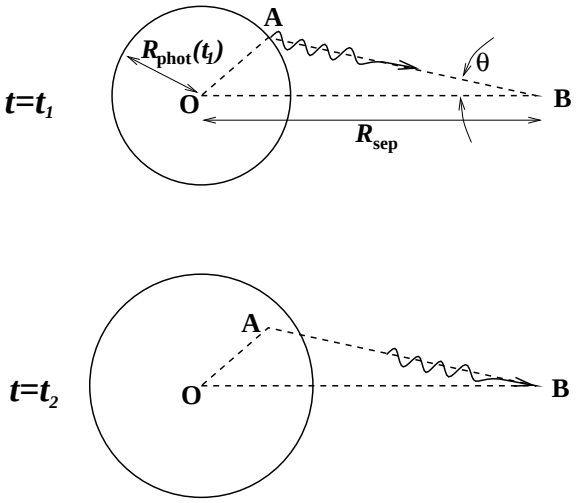

Figure 3: Emission of a photon from point A on the photosphere at time $t = t_1$, and reception of the photon at point B at time $t = t_2$. Point O is the centre of the SN explosion.

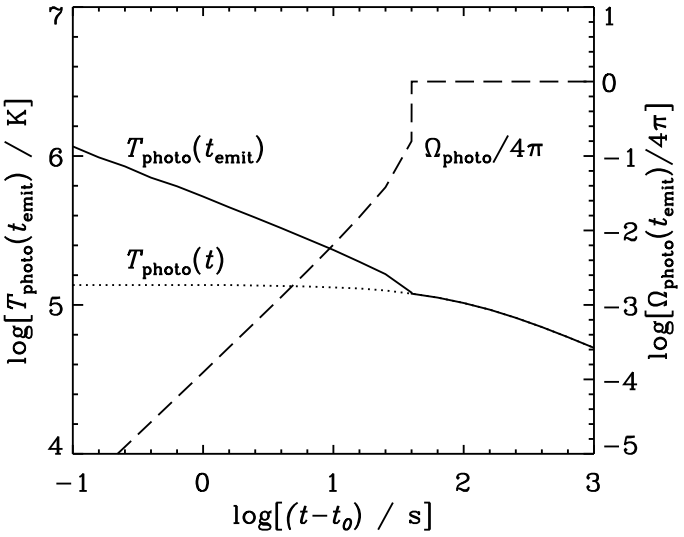

Figure 4: Temperature and solid angle subtented by photosphere as would be observed from distance $r = 3.4 \times 10^{12}$ cm, as a function of time delay following arrival of fastest matter.

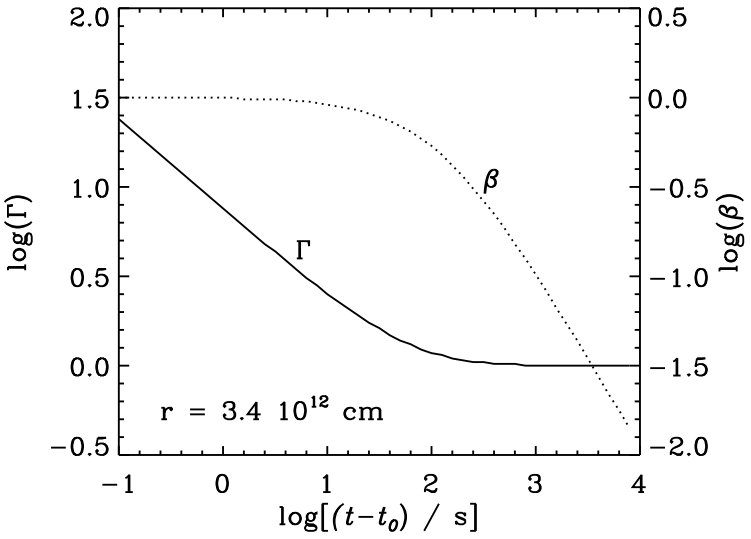

Figure 5: Lorentz Γ and β of matter arriving at distance $r = 3.4 \times 10^{12}$ cm as a function of time delay following arrival of fastest matter.

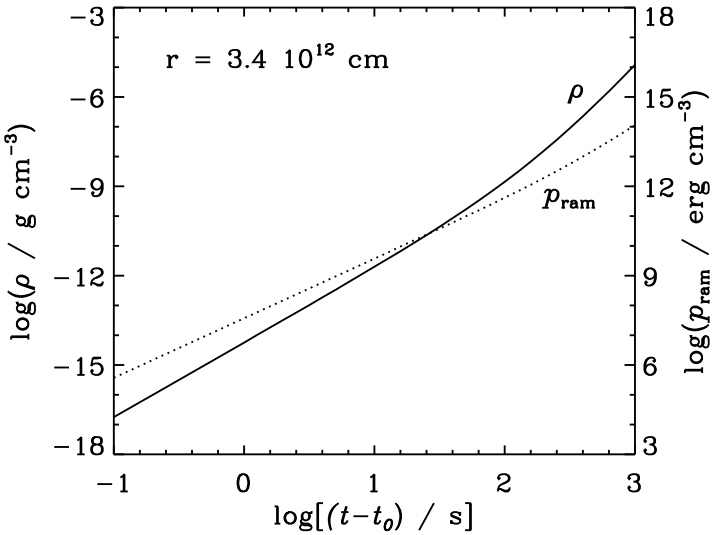

Figure 6: Density and ram pressure of matter arriving at distance $r = 3.4 \times 10^{12}$ cm as a function of time delay following arrival of fastest matter.

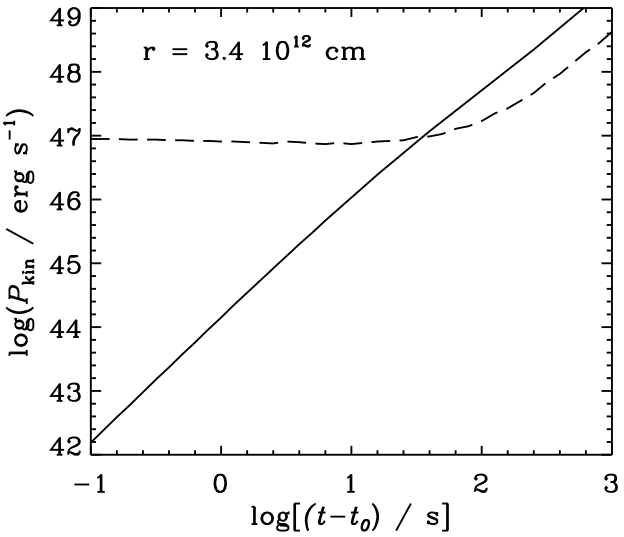

Figure 7: Kinetic energy flux of matter arriving at distance $r = 3.4 \times 10^{12}$ cm as a function of time delay following arrival of fastest matter (solid curve). The dashed curve shows the effect multiplying by the fraction $k \approx 0.2$ intercepted by area $\pi R_{\rm star}^2$ for $R_{\rm star} = 10^{12}$ cm, and multiplying by a beaming factor $2/(1 - \cos\theta_{\rm beam})$ where $\theta_{\rm beam} \approx 1/\sqrt{2}\Gamma^2$ (see text).

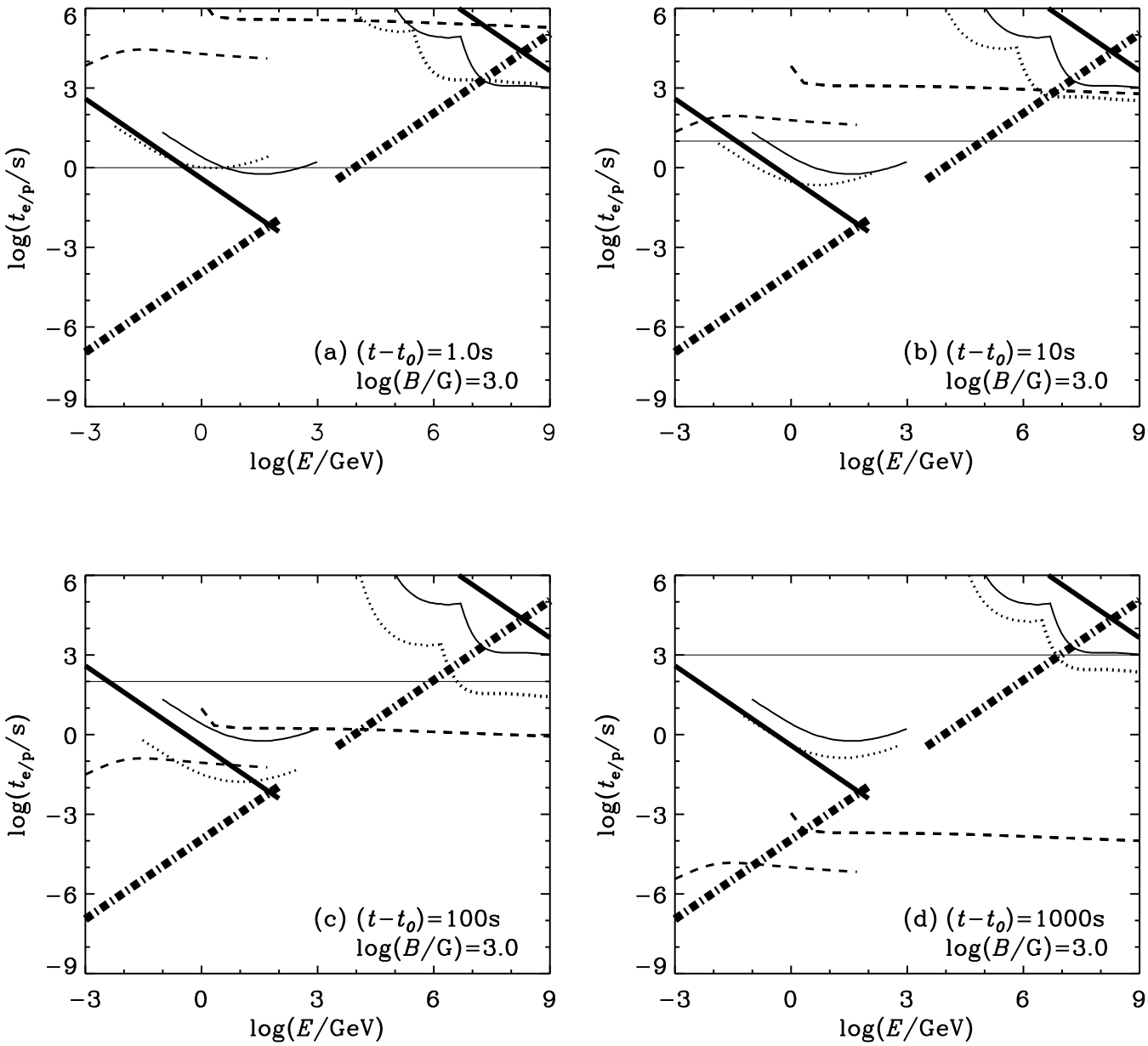

Figure 8: Acceleration time for $B = 10^3$ G and $\xi = 10^{-3}$ (thick chain line), energy loss time scales for various processes, and the time available for acceleration/losses (thin horizontal line) are shown for distance $r = 3.4 \times 10^{12}$ cm as a function of energy for time delays of (a) $(t - t_0) = 1$ s, (b) 10 s, (c) 100 s and (d) 1000 s. The energy loss/interaction processes shown are: synchrotron loss by electrons (thick solid line at left), synchrotron loss by protons (thick solid line at right), ionization/bremsstrahlung loss of electrons (dashed curve on left), hadronic interactions of protons with nuclei (dashed curve on right), inverse Comption scattering of electrons on 3×10^4 K starlight (thin solid curve on left), Bethe-Heitler pair production interactions and pion photoproduction interactions of protons on 3×10^4 K starlight (thin solid curve on right), inverse Comption scattering of electrons on thermal SN radiation (thin dotted curve on left), Bethe-Heitler pair production interactions and pion photoproduction interactions of protons on thermal SN radiation (thin dotted curve on right).

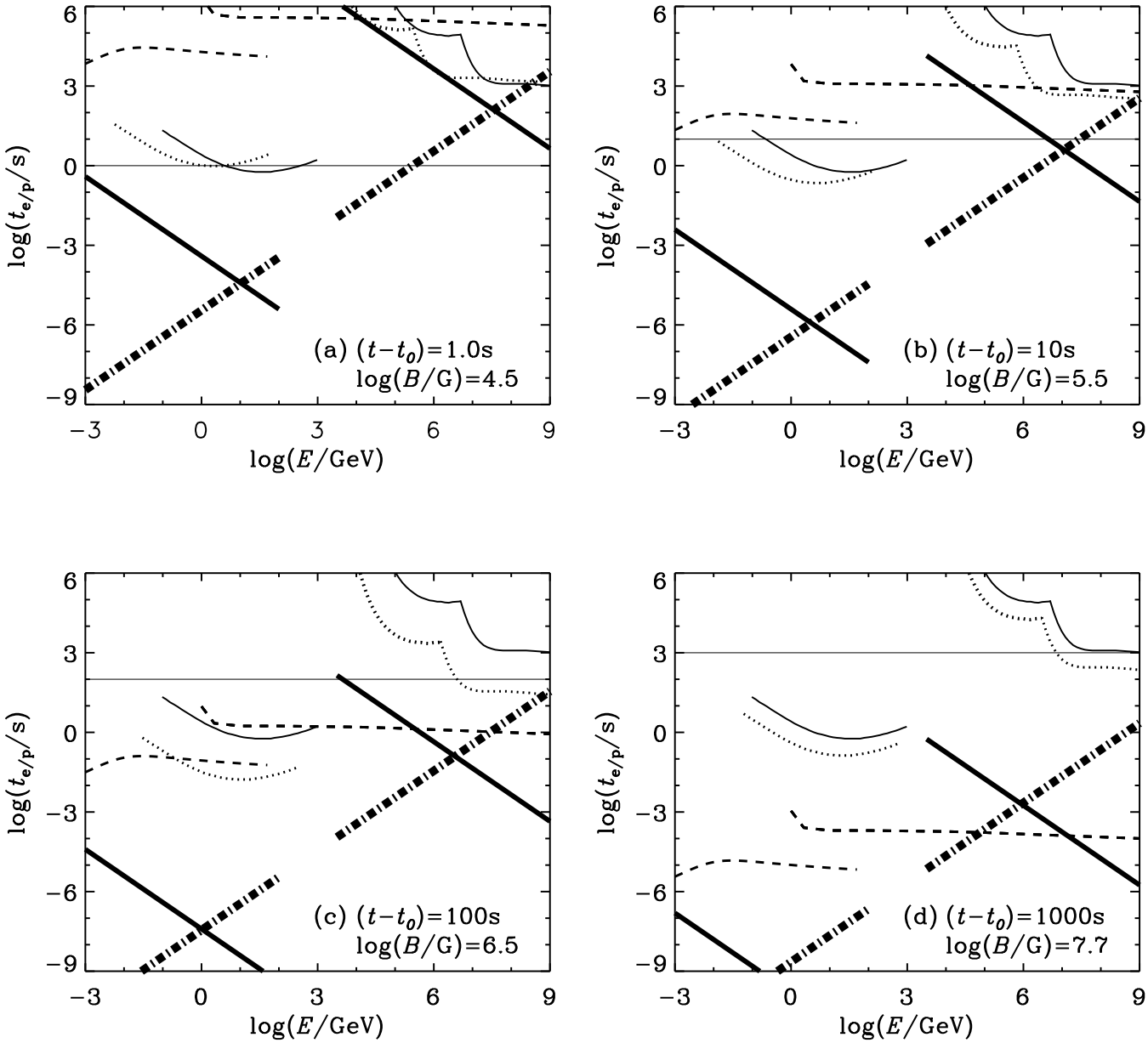

Figure 9: Acceleration time for $B^2/8\pi = p_{\rm ram}$ and $\xi = 10^{-3}$ (thick chain line), energy loss time scales for various processes and the time available for acceleration/losses (thin horizontal line) at distance $r = 3.4 \times 10^{12}$ cm as a function of energy for time delays of (a) $(t - t_0) = 1$ s, (b) 10 s, (c) 100 s and (d) 1000 s. The energy loss/interaction processes shown are as desribed in Fig. 8.

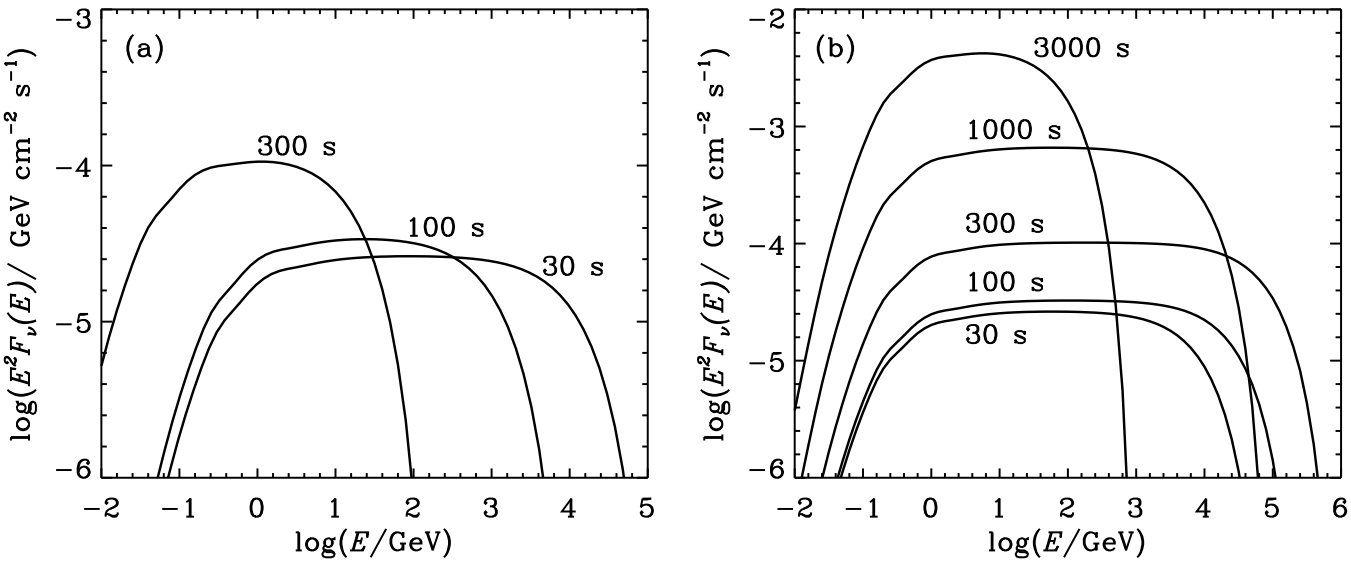

Figure 10: Predicted $(\nu_\mu + \bar{\nu}_\mu)$ flux at various times for (a) $B = 10^3$ G, and (b) $B^2/8\pi = p_{\rm ram}$.

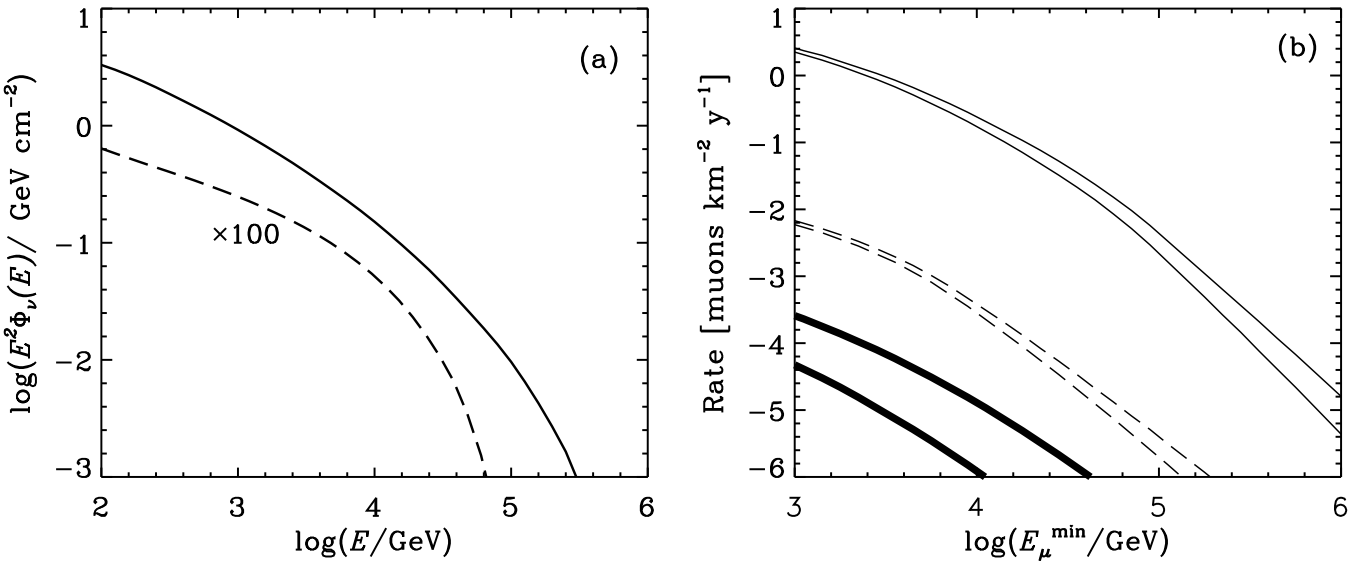

Figure 11: (a) Predicted $(\nu_\mu + \bar{\nu}_\mu)$ flux fluence for $B = 10^3$ G multiplied by 100 (dashed curve), and $B^2/8\pi = p_{\rm ram}$ (solid curve). (b) Muon signal corresponding to the fluences given in part (a) together with the atmospheric background during 100 s arriving within 5° of the GRB direction (thick solid curves). The upper curves give the signal expected if the source direction is horizontal, and the lower curves give the signal expected if the source direction is in the vertically downward direction.